J. Fluid Mech. (2004), *vol.* 513, *pp.* 265–286.
DOI: 10.1017/S0022112004000059 Printed in the United Kingdom

Stress and configuration relaxation of an initially straight flexible polymer

By P. DIMITRAKOPOULOS

Department of Chemical Engineering, University of Maryland, College Park, MD 20742, USA

(Received 1 May 2003 and in revised form 15 April 2004)

The stress and conformational relaxation of an initially straight flexible polymer is studied through Brownian dynamics simulations covering a broad range of time scales and polymer lengths. At short times $t \ll N^{-2}$, the strong stress component scales as $\sigma_{11} \sim N^3$ ('1' is the direction of the original alignment), while the weak component is $\sigma_{22} \sim N$ (where N is the polymer length). At intermediate times $N^{-2} \ll t \ll N^2$, the stress decay is shown to be anisotropic: $\sigma_{11} \sim N^2 t^{-1/2}$ while $\sigma_{22} \sim N^{1/2} t^{-1/4}$. At long times $t \gg N^2$, both stress components show the same exponential decay associated with the reduction of the chain's length, while their magnitudes are still different; $\sigma_{11} = O(N)$ while $\sigma_{22} = O(1)$. The configuration relaxation is studied over the same extended time periods by employing scaling laws for the evolution of the eigenvalues of the gyration tensor. After the short-time free diffusion, the configuration relaxation is anisotropic at intermediate times: the chain's width grows as $R_\perp \sim N^{-1/4} t^{3/8}$ while its length is reduced as $R_\parallel(0) - R_\parallel \sim t^{1/2}$. During long times, the polymer length shows an exponential decay towards the equilibrium coil-like shape. The polymer chain remains aligned along the original direction until late in long times where the chain rotation is shown to be significant. The chain is shown to be far from equilibrium during the entire transient relaxation. By focusing on the chain's longitudinal relaxation, a quasi-steady equilibrium of the link tensions in shown to exist along the chain's length; the mechanism is identical to that found in Grassia & Hinch (1996) based on a sideways motion model. This mechanism also explains the ability of the FENE model to describe the longitudinal relaxation of the flexible bead-rod chain. A comparison with experimental findings from initially straight single tethered DNA molecules is also included.

1. Introduction

The present study considers the relaxation of a single flexible polymer chain from an initial straight configuration in a viscous solvent. Physically, this problem may correspond to the case of a polymer chain fully stretched by an (infinitely) strong flow and then relaxed by switching the flow off. This problem is also motivated by recent experiments with single DNA molecules relaxing after being fully extended by applied forces as well as by the recent development of micro-devices involving stretched tethered biopolymers (e.g. Perkins *et al.* 1994, 1999; Wuite *et al.* 2000). As is well known, large stresses are developed even in dilute polymer solutions involving fully stretched polymer chains (Doyle *et al.* 1998). Thus, our interest lies in understanding the mechanisms of relaxation of these stresses. In this article, we present the stress relaxation over a broad range of time scales and polymer lengths. We also study the configuration relaxation which causes the relaxation of stress over

the same time periods and polymer lengths. From a theoretical point of view, the present problem is further motivated by the fact that the experiment starts with a straight configuration (i.e. a chain configuration far from equilibrium) and moves towards the equilibrium coil-like shape. The interest lies not only on the chain's properties far from equilibrium, but also on how the chain approaches equilibrium.

Based on previous studies (Grassia & Hinch 1996, hereinafter referred to as GH; Doyle *et al.* 1997, 1998), we have a good idea of the polymer relaxation. Immediately after the chain is left to relax from the straight configuration, the transverse component of the tension force on each bead is much smaller than the corresponding component of the Brownian forces, and the beads show a free diffusion (the mean-square sideways displacement scales with time t). As the transverse tension forces increase with time, they balance the Brownian forces and the free transverse bead diffusion is arrested; this happens at times $t \sim N^{-2}$ where N is a dimensionless expression for the polymer length (i.e. the number of links). At intermediate times, a quasi-static balance between link tension and bead diffusion produces a mean-square transverse link growth of $t^{1/2}$ (GH). At the straight configuration, the strong stress component along the direction of the initial extension scales as N^3 and remains constant at short times, while it shows a power law decay $t^{-1/2}$ at intermediate times. Finally, at long times, the stress shows a Rouse-like exponential decay towards equilibrium with a relaxation rate higher than that predicted by the Rouse model (GH; Doyle *et al.* 1997).

We note that the previous studies report only on the strong component σ_{11} of the polymer stress (where '1' is the direction of the initial extension) (GH), or on the stress difference $\sigma_{11} - \sigma_{22}$ which scales as σ_{11} (Doyle *et al.* 1997, 1998), with rather limited investigation of the configuration relaxation. In this study, we investigate again the relaxation of the strong stress σ_{11} over a much broader range of time scales and polymer lengths. In addition, the entire relaxation of the weak stress component σ_{22} is presented, which follows a different power law decay at intermediate times, i.e. the stress decay is anisotropic at these times (see § 3). Although for an incompressible fluid only the stress difference is meaningful, knowledge of both components of the polymer stress helps us understand better the polymer relaxation. In particular, the anisotropy in the stress decay suggests a corresponding anisotropy in the configuration relaxation (as shown in § 4).

We also provide a detailed study of the configuration relaxation in § 4. To the best of our knowledge, so far, the configuration relaxation has been monitored for short chains and times only, i.e. for periods much shorter than those of the polymer stress, owing to a shortage of appropriate configuration functions. In this study, we present both the longitudinal and transverse conformational relaxation for the same extended time periods and polymer lengths as our results for the stress relaxation. We achieve this by employing scaling laws for the relaxation of the eigenvalues of the gyration tensor; their evolution is shown to be an appropriate measurement of the configuration evolution for the entire chain and its impact on the stress relaxation. The configuration relaxation is concluded by studying the rotation of the entire chain and the motion of the chain's centre of mass.

Our numerical results for the conformational evolution of the polymer chain reveal that over an extended intermediate-time period the chain shows a different power-law transverse evolution ($t^{3/4}$) than that of the links ($t^{1/2}$). The chain's longitudinal relaxation is also studied over the entire polymer relaxation. Based on our results for the longitudinal relaxation, a quasi-steady equilibrium of the tension forces in the longitudinal direction is shown to exist at intermediate times; the mechanism is identical to that found in Grassia & Hinch (1996) based on a sideways motion

model. This mechanism is in agreement with the recent findings of Ghosh *et al.* (2001) where the longitudinal force along a Cramer's chain was numerically determined as a function of the chain length and was shown to follow the predictions of the FENE model during relaxation (as discussed in § 5.2). The polymer chain is shown to be far from equilibrium even at the long times of transient dynamics, while it should approach equilibrium near the end of the long-time behaviour where monitoring transient properties produces results indistinguishable from the noise of the Brownian motion.

We conclude our study by comparing our numerical results with the experimental findings from initially straight single tethered DNA molecules (Perkins *et al.* 1994). Our results are in excellent qualitative agreement with these experiments and suggest a detailed study of tethered polymers.

2. Mathematical formulation

A discretized version of the flexible wormlike chain model (e.g. Doi & Edwards 1996; Yamakawa 1997) is employed based on a Brownian dynamics method developed in Grassia & Hinch (1996). This method considers a bead-rod model with fixed bond lengths and ignores hydrodynamic interactions among beads as well as excluded-volume effects. The polymer chain is modelled as $N_B = (N+1)$ identical beads connected by N massless links of fixed length b (which is used as the length unit). The position of bead i is denoted as $\boldsymbol{X}_i$, while the link vectors are given by $\boldsymbol{d}_i = \boldsymbol{X}_{i+1} - \boldsymbol{X}_i$. For a fixed b, the properties of the polymer chain are specified by the (constant) contour length of the chain L or equivalently by the number of links N.

Assuming that the bead inertia is negligible, the sum of all forces acting on each bead i must vanish, which leads to the following Langevin equation

$$\zeta \frac{\mathrm{d}\boldsymbol{X}_i}{\mathrm{d}t} = \boldsymbol{F}_i^{rand} + \boldsymbol{F}_i^{ten} + \boldsymbol{F}_i^{cor}, \tag{1}$$

where the friction coefficient ζ is assumed to be uniform (GH). $\boldsymbol{F}_i^{rand}$ is the Brownian force due to the constant bombardments of the solvent molecules. The force $\boldsymbol{F}_i^{ten} = T_i \boldsymbol{d}_i - T_{i-1}\boldsymbol{d}_{i-1}$, where T_i is a constraining tension along the direction of each link $\boldsymbol{d}_i$, ensures the link inextensibility. Finally, $\boldsymbol{F}_i^{cor}$ is a corrective potential force added so that the equilibrium probability distribution of the chain configurations is Boltzmann (Fixman 1978; GH). The resulting system of equations may be solved in $O(N)$ operations (GH). Ensemble averages are determined by employing 10^4 to 10^5 independent initial configurations. All properties presented in this paper are calculated as, and refer to, the ensemble averages of the corresponding instantaneous values. Thus, the polymer stress refers to the ensemble-averaged polymer stress (and not to the instantaneous value) while the three eigenvalues of the gyration tensor presented below are calculated as ensemble averages of the instantaneous values of the eigenvalues.

The Brownian forces give rise to a microscopic time scale associated with the diffusive motion of one bead, $\tau_{rand} = \zeta b^2 / k_B T$, which is used as the unit for the times reported in this work if no other unit is used. The polymer stress $\boldsymbol{\sigma} = -\sum_{i=1}^{N+1} \boldsymbol{X}_i \, \boldsymbol{F}_i^{total}$, where $\boldsymbol{F}_i^{total}$ is the sum of all forces appearing on the right-hand side of (1), is calculated efficiently by eliminating the fluctuating terms of large magnitude which produce vanishing expectation values, as discussed in Grassia & Hinch (1996). In the following sections, we present the polymer stress in units of $k_B T$. The numerical method employed in this work has been used to study semiflexible polymers near

equilibrium (Dimitrakopoulos, Brady & Wang 2001) and will not be discussed further in the present paper.

3. Stress relaxation

Forcing a flexible polymer chain to obtain a straight configuration, the polymer accumulates only normal stresses which decay as the chain relaxes towards the equilibrium coil-like shape. Assuming that '1' is the direction of the initial configuration, the strong component of the normal stress is σ_{11}, while the other two components are equal, $\sigma_{22}=\sigma_{33}$, owing to symmetry. Also, no shear stress develops in our system (i.e. $\sigma_{ij}=0$ for any $i\neq j$). At equilibrium, the stress is simply $\boldsymbol{\sigma}=-\boldsymbol{I}$ (where $\boldsymbol{I}$ is the unit 3×3 matrix, e.g. $\sigma_{11}=\sigma_{22}=-1$) owing to the motion of the centre of mass (as discussed at the end of § 4). Subtracting the equilibrium value, the two independent non-zero components of stress (σ_{11} and σ_{22}) have opposite signs since in the '1' direction the polymer chain is being compressed while in the other two directions the chain is being extended. (Based on the way we define the stress, $\sigma_{11}+1>0$ while $\sigma_{22}+1<0$.) Thus in the figures below, we plot the strong component as $(\sigma_{11}+1)$, and the weak component as $-(\sigma_{22}+1)$. The polymer length may be presented by either the number of beads N_B or the number of links N. Obviously, for long enough chains, there is no difference; but for small to moderate length chains, the difference may be significant. Thus in the figures below, we use that number which produces the best fitting in the scaling laws with the understanding that for long enough chains there is no distinction. A discussion on the time scale for the stress relaxation of discrete chains at intermediate and long times will be included in due course.

Figure 1 shows the stress relaxation at early times, for chains with length varying from $N=5$ to 400. For each length, the stress relaxation is determined for a short time period only, enabling us to study very long chains. On the other hand, by the use of scaling laws, these curves can reveal the polymer behaviour over broad time periods as shown below. The curves for small chain lengths ($N=5$, 10, 20) reveal the entire stress relaxation: at early times there is a plateau since no stress relaxation is significant yet; after the plateau, the appearance of a power law decay is evident at intermediate times; and, finally, there is an exponential decay at long times. As the figure shows, the stress of a straight chain is higher for longer chains while both stress components, σ_{11} and σ_{22}, show the same qualitative behaviour.

The scaling behaviour for the magnitude of the initial stress and the initial decay is shown in figure 2, where, after replotting our data, all curves fall on each other at short times. Thus, initially $\sigma_{11}\sim N^3$ while its exact value is in excellent agreement with the prediction of $N(1/3\,N^2+N+5/3)-(N+1)$ presented in the work of Grassia & Hinch (1996). The other stress component is exactly $\sigma_{22}=-(N+1)$, revealing that this component is much weaker, i.e. the large stresses developed in dilute polymer solutions under extensional flows are mainly associated with the strong σ_{11} component. The strong stress component results from the requirement to maintain link inextensibility; i.e. σ_{11} is caused by $O(N^2)$ link tensions over N links (GH). The weak stress component σ_{22} results from the transverse component of the Brownian forces, i.e. $O(1)$ stresses per link over N links. (More details are given in § 5.) This figure also reveals that the initial decay from the plateau occurs at times $t\sim N^{-2}$ for both stress components.

The stress relaxation at intermediate times is shown in figure 3, where after replotting the same data as before, a power law decay is clearly evident over several time decades. In particular, the strong stress component σ_{11} shows a power law decay

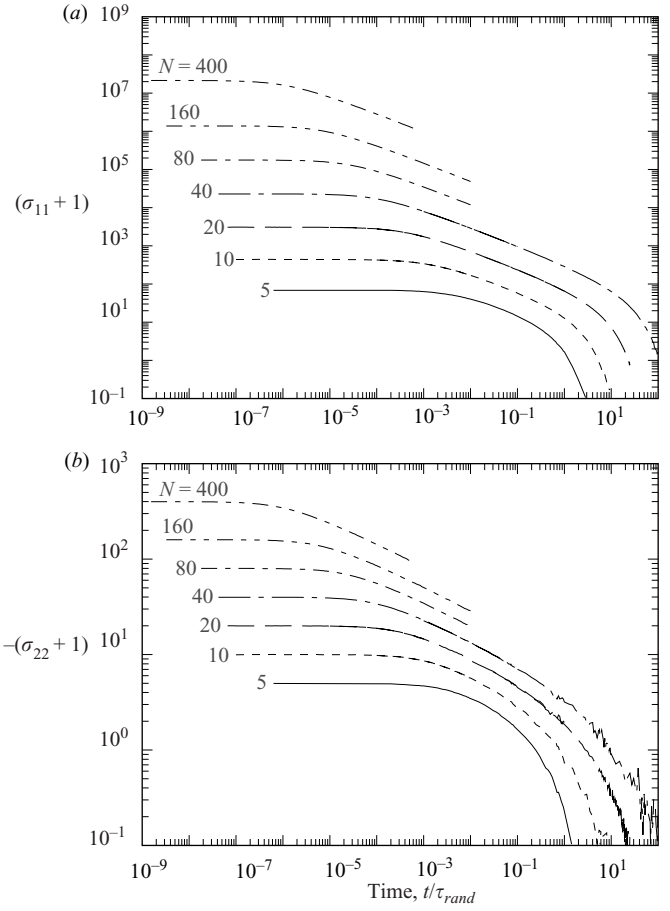

FIGURE 1. Relaxation of the polymer chain at short times. (*a*) Stress component $(\sigma_{11}+1)$ versus time for polymer length $N = 5, 10, 20, 40, 80, 160, 400$. (*b*) As in (*a*) but for the stress component $(\sigma_{22}+1)$. (Note that this stress component is negative.)

of $t^{-1/2}$ while the weak component σ_{22} decays as $t^{-1/4}$. Thus, an anisotropy in the stress relaxation is observed at intermediate times. We note that in the work of Grassia & Hinch (1996) the numerical results for σ_{11} in their figure 6 were rather limited, while in Doyle *et al.* (1998) a clear power law decay $t^{-1/2}$ was shown in their figure 4 for $\sigma_{11} - \sigma_{22} \sim \sigma_{11}$. In our figure 3, beyond the clear evidence of the power law decay over several time decades, the new information provided is the behaviour of the weak stress component σ_{22} as well as our preference for the time scale.

In particular, in figure 3 the time has been scaled with τ_{nmode} which is the exact value of the time scale for the relaxation of the first normal mode (and for the long-time relaxation of the end-to-end vector) of the Rouse model,

$$\tau_{nmode} = \tau_{rand} \left[12 \sin^2 \left(\frac{\pi}{2(N+1)} \right) \right]^{-1}. \tag{2}$$

By employing this value for the time scale, we avoid possible misfitting of the data for small and moderate chain length N. For large N, $\tau_{nmode} = \tau_{rand}\, N^2/(3\pi^2)$; thus, based

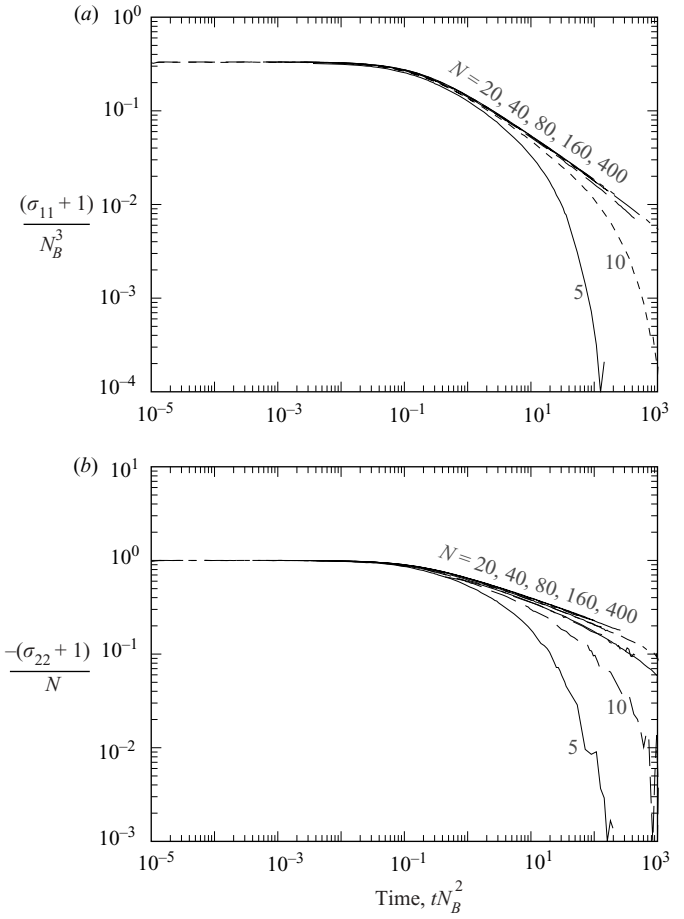

FIGURE 2. Scaling law for the stress relaxation at short times. (*a*) Stress component $(\sigma_{11}+1)$ scaled with N_B^3 versus time t scaled with N_B^{-2} for polymer length $N = 5, 10, 20, 40, 80, 160, 400$. (*b*) As in (*a*) but for the stress component $(\sigma_{22}+1)$ scaled with N.

on our figure at intermediate times the polymer stress is

$$\frac{\sigma_{11}}{N} \sim \left(\frac{t}{N^2}\right)^{-1/2} \quad \text{or} \quad \sigma_{11} \sim N^2 t^{-1/2}, \tag{3}$$

$$\sigma_{22} \sim \left(\frac{t}{N^2}\right)^{-1/4} \quad \text{or} \quad \sigma_{22} \sim N^{1/2} t^{-1/4}. \tag{4}$$

At long times, the polymer stress is expected to follow a Rouse-like exponential decay towards equilibrium. Based on numerical results, Grassia & Hinch (1996) reported that at long times $\sigma_{11} \sim N \exp(-70.2t/N^2)$ or $N \exp(-2.4t/\tau_{nmode})$. The same result was reported for $(\sigma_{11} - \sigma_{22})$ in Doyle *et al.* (1997). Based on these results, the bead-rod model shows a faster exponential decay than that predicted by the Rouse model, $(\sigma_{11})_{Rouse} \sim \exp(-6\pi^2 t/N^2)$ or $\exp(-2t/\tau_{nmode})$. Figure 4 shows the stress relaxation at long times for chains with length varying from $N = 5$ to 40. As this figures reveals, both stress components show an exponential decay $\sim \exp(-2.3t/\tau_{nmode})$, faster than that predicted by the Rouse model and in good agreement with the previous

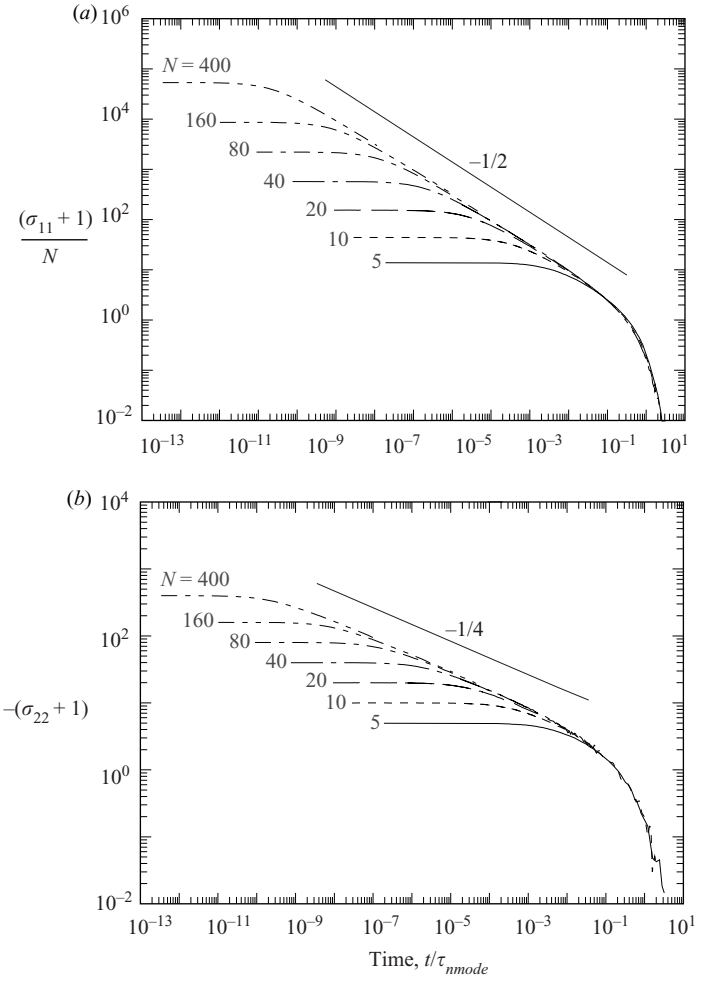

FIGURE 3. Scaling law for the stress relaxation at intermediate times. (*a*) Stress component $(\sigma_{11}+1)$ scaled with N versus time t scaled with τ_{nmode} for polymer length $N = 5, 10, 20, 40, 80, 160, 400$. (*b*) As in (*a*) but for the stress component $(\sigma_{22}+1)$ unscaled.

numerical studies. (Note that the slope of -1 shown in figure 4 has been multiplied by $\ln 10 \approx 2.3$.) In addition, the strong stress component is $\sigma_{11} = O(N)$, while the weak component is $\sigma_{22} = O(1)$. (The small expectation value of σ_{22} results in an increased noise in the numerical results in figure 4*b*.) We emphasize again that by scaling our data at long times with the exact value of τ_{nmode}, we avoid misfitting of curves for small values of N as commonly happens when the time scale N^2 (valid for long chains $N \gg 1$) is employed.

As a closure for this section, we show that simple scaling arguments can predict the stress relaxation at intermediate times. In particular, the strong stress component is $\sigma_{11} = O(N^3)$ at short times $t = O(1/N^2)$, while $\sigma_{11} = O(N)$ at long times $t = O(N^2)$. Matching these two stresses at intermediate times with a single power law t^a gives

$$(\sigma_{11})_{short} = N^3(N^2 t)^a \;=\; (\sigma_{11})_{long} = N\left(\frac{t}{N^2}\right)^a, \tag{5}$$

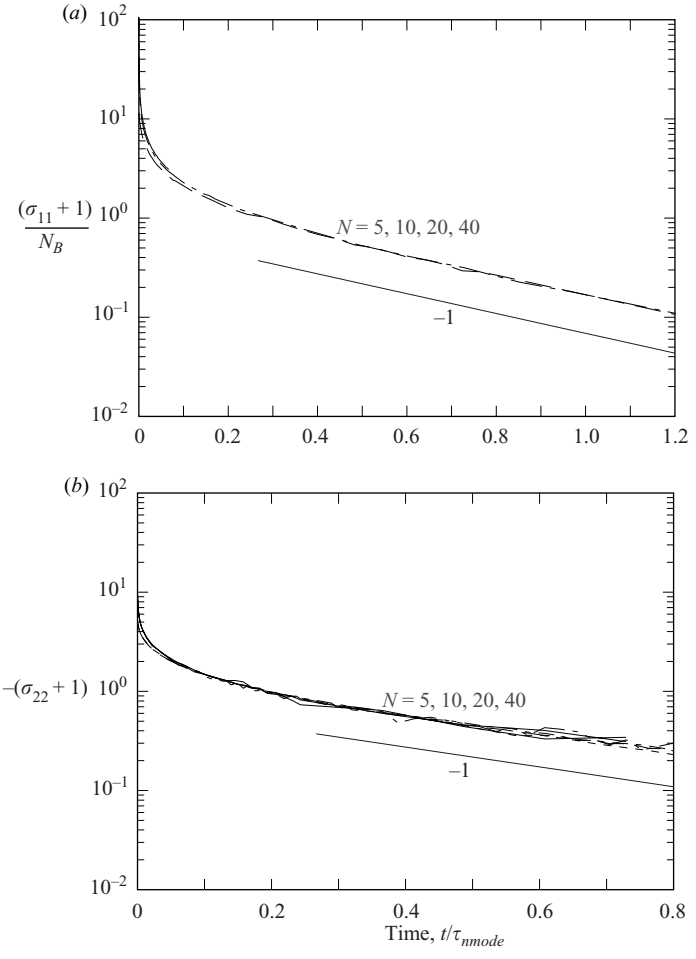

FIGURE 4. Scaling law for the stress relaxation at long times. (*a*) Stress component $(\sigma_{11}+1)$ scaled with N_B versus time t scaled with τ_{nmode} for polymer length $N = 5, 10, 20, 40$. (*b*) As in (*a*) but for the stress component $(\sigma_{22}+1)$ unscaled.

which is only valid for $a = -1/2$ (as also shown in GH) and thus at intermediate times $\sigma_{11} \sim N^2 t^{-1/2}$, in agreement with our numerical results shown in figure 3(*a*). Similarly, the weak stress component is $\sigma_{22} = O(N)$ at short times and $\sigma_{22} = O(1)$ at long times. Matching these two stresses at intermediate times with a single power law t^b gives

$$(\sigma_{22})_{short} = N(N^2 t)^b \;=\; (\sigma_{22})_{long} = 1\left(\frac{t}{N^2}\right)^b, \tag{6}$$

which is only valid for $b = -1/4$ and thus at intermediate times $\sigma_{22} \sim N^{1/2} t^{-1/4}$ as shown in figure 3(*b*).

Studying the two components of the polymer stress separately, two conclusions may be derived. First, the anisotropy in the stress relaxation suggests a corresponding anisotropy in the configuration relaxation. This issue is being pursued further in the following section. Secondly, the different magnitude of the two stresses suggests that

the polymer chain is far from equilibrium during the entire transient relaxation as discussed further in § 5.

4. Configuration relaxation

Studying the relaxation of the polymer configuration is essential to understand the configuration's impact on the properties of the polymeric solution including the polymer stress. Previous studies have tried to do this by employing several conformational functions. For the current problem, the transverse evolution of the polymer chain at intermediate times was determined by monitoring the transverse motion of the central bead in the chain (Grassia & Hinch 1996) or the motion of individual beads along the chain (Doyle *et al.* 1997). In both studies, the monitoring was restricted to short time periods. In this paper, we follow a different path considering new conformational functions and, by using the scaling law methodology, we present the configuration evolution over the same time period as that for our stress relaxation while we determine the configuration's dependence on both time t and polymer length N. We are also interested in studying the entire configuration relaxation of the chain including its transverse and longitudinal relaxation, its rotational relaxation and the motion of the centre of mass.

To analyse the evolution of the polymer chain we calculate the eigenvalues of the gyration tensor

$$\boldsymbol{R}_G^2 = \frac{1}{N+1}\sum_{i=1}^{N+1}(\boldsymbol{X}_i - \boldsymbol{X}_c)(\boldsymbol{X}_i - \boldsymbol{X}_c), \tag{7}$$

where $\boldsymbol{X}_c = \sum_{i=1}^{N+1} \boldsymbol{X}_i/(N+1)$ is the centre of mass of the chain. The first (largest) eigenvalue measures the size of the chain along its major axis (i.e. the chain's length), and may be used to study the longitudinal reduction of the polymer chain. The other two eigenvalues measure the size of the chain along its two minor axes (i.e. the chain's width), and may be used to study the transverse evolution of the polymer chain. These conformational functions involve all length scales, from that of the single bead to the length scale of the entire chain, and thus can be used to describe the polymer evolution over extended time periods.

Figure 5(a) shows the evolution of the second eigenvalue $R_{G,2}^2$ for two representative chain lengths, $N = 5$ and 160. (The evolution of the third eigenvalue $R_{G,3}^2$ is similar and has been omitted.) The results for small N reveal the entire transverse relaxation of the polymer chain. At short times, the beads show a free diffusion, i.e. $R_{G,2}^2 \sim t$. At intermediate times, a slower transverse displacement is observed. For $N = 5$, the intermediate-time behaviour is limited, but it is extended for longer chains; as this figure reveals, for $N = 160$, the second eigenvalue $R_{G,2}^2$ shows a growth of $t^{3/4}$. Finally, at long times, no transverse configuration relaxation is observed; the polymer transverse configuration has reached equilibrium and the evolution of $R_{G,2}^2$ shows a plateau. The final value of $R_{G,2}^2$ is predicted well by the results of Kranbuehl & Verdier (1977), i.e. $(R_{G,2}^2)_{eq} = 0.176\,(R_G^2)_{eq} \sim Nb^2$. We emphasize that the described behaviour is based not only on the two values of polymer length shown in figure 5(a), but also on our full set of values (i.e. $N = 5$, 10, 20, 40, 160, 400) which are omitted in this figure for clarity (but included in figure 5b).

To further investigate the most interesting intermediate-time behaviour, it is still computationally impractical to study a long polymer chain for an extended time period. Clearly, a scaling law should be used to match the behaviour of chains with

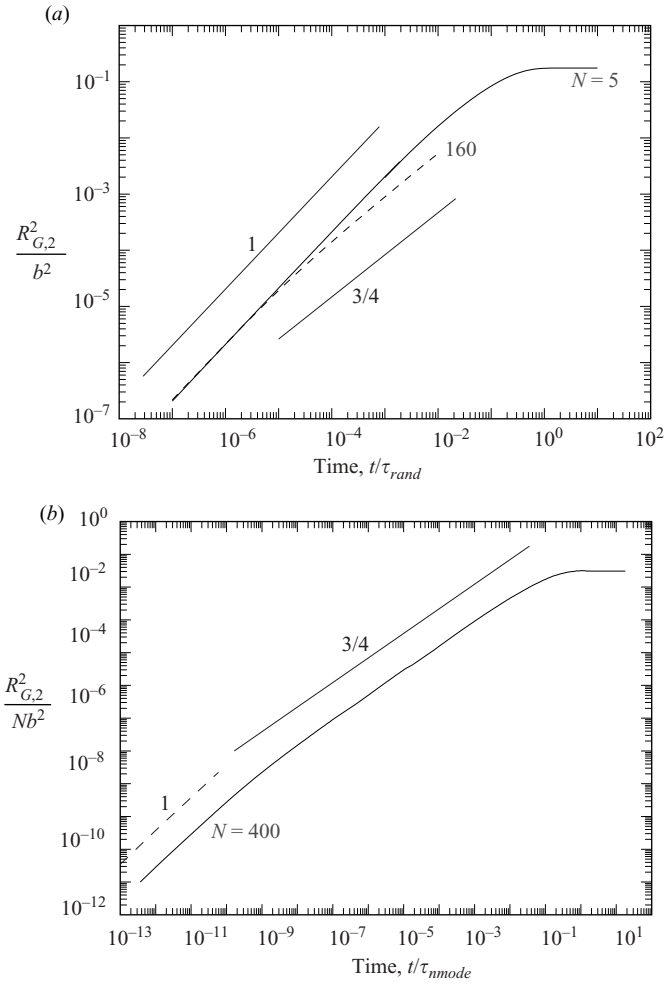

FIGURE 5. Transverse evolution of the polymer chain. (*a*) Evolution of the second eigenvalue $R^2_{G,2}$ of the gyration tensor for two representative chain lengths $N = 5, 160$. This figure also reveals the scaling law for $R^2_{G,2}$ at short times. (Our results for $N = 10, 20, 40, 400$ have been omitted for clarity.) (*b*) Scaling law for the evolution of $R^2_{G,2}$ at intermediate times. This curve was generated by employing chains with $N = 5, 10, 20, 40, 160, 400$.

different lengths. This idea is employed in figure 5(*b*) where we present the evolution of the second eigenvalue $R^2_{G,2}$ for our full set of polymer lengths, scaling $R^2_{G,2}$ with N at long times) and the time t with τ_{nmode}. (Note that N and τ_{nmode} are the scales of $R^2_{G,2}$ and t, respectively, at the end of the intermediate-time behaviour.) As this figure reveals, at intermediate times the chain's width shows a clear growth,

$$\frac{R^2_{G,2}}{N} \sim \left(\frac{t}{N^2}\right)^{3/4} \quad \text{or} \quad R^2_{G,2} \sim N^{-1/2}\, t^{3/4}, \tag{8}$$

over several time decades.

The transition from the short-time to the intermediate-time behaviour and the configuration evolution at intermediate times were first studied by Grassia & Hinch

(1996). By assuming a quasi-static balance between the tension forces and the transverse diffusive forces on the beads, the authors determined the transverse link growth and from that they predicted a mean-square transverse bead (and chain) motion growing as $t^{1/2}$. This seems to contradict our results for the evolution of the two minor eigenvalues of the gyration tensor. Assuming that our numerical results are correct, the difference should result from the simplification the authors had to employ to connect the transverse evolution of beads with that of links, i.e. by assuming that the typical wavelength of the transverse bead displacement is $O(N)$. We note that GH supported their theoretical analysis by numerically determining the transverse evolution of the middle bead, but their results are limited, valid only for a short time period and for short chains, i.e. from $N=4$ to 12 as shown in their figure 7. Our conclusion is also supported by the results of Doyle *et al.* (1997), who numerically calculated the transverse diffusion of individual beads along a single chain with 50 beads and found a growth rate of $t^{3/4}$ over two time decades (as shown in their figure 14). Furthermore, our numerical results are supported by simple scaling arguments. Similarly to the stress, given the transverse growth of the polymer chain for short and long times, scaling arguments predict that the observed power law at intermediate times is the simplest power law which can match the transverse growth at short and long times. Observe that at short times $t=O(1/N^2)$ the chain's width is $R^2_{G,2}=O(N^{-2})$, while $R^2_{G,2}=O(N)$ at long times $t=O(N^2)$. Matching these two magnitudes at intermediate times with a single power law t^a gives

$$\left(R^2_{G,2}\right)_{short}=N^{-2}\,(tN^2)^a=\left(R^2_{G,2}\right)_{long}=N\left(\frac{t}{N^2}\right)^a, \tag{9}$$

which is only valid for $a=3/4$ and, thus, at intermediate times $R^2_{G,2}\sim N^{-1/2}t^{3/4}$ in agreement with our numerical results shown in figure 5(*b*).

We now turn our attention to the longitudinal length of the polymer chain and present the reduction of the first eigenvalue $R^2_{G,1}$ of the gyration tensor with respect to its initial value in figure 6. This figure reveals that at short times the chain length is reduced as $\Delta R^2_{G,1}\equiv R^2_{G,1}(0)-R^2_{G,1}(t)\sim N^2t$, while at intermediate times it is reduced as

$$\frac{\Delta R^2_{G,1}}{N^2}\sim\left(\frac{t}{N^2}\right)^{1/2}\quad\text{or}\quad R^2_{G,1}(0)-R^2_{G,1}(t)\sim Nt^{1/2}. \tag{10}$$

We note that at the end of short times $\Delta R^2_{G,1}=O(1)$ while at the end of intermediate times $\Delta R^2_{G,1}=O(N^2)$. Thus, during both short and intermediate times, the chain's length has a magnitude of $R^2_{G,1}=O(N^2)$, i.e. the polymer chain is practically straight. This conclusion is shown clearly in figure 7(*a*) where we replot our results for the first eigenvalue $R^2_{G,1}$ with respect to its value at equilibrium, $(R^2_{G,1})_{eq}=0.76\,(R^2_G)_{eq}$ (Kranbuehl & Verdier 1977). In addition, at times $t\sim\tau_{nmode}$, the chain shows a sharp decrease in the average polymer length; as revealed in figure 7(*b*), at long times, the polymer length shows an exponential decay

$$\delta R^2_{G,1}(t)\equiv R^2_{G,1}(t)-\left(R^2_{G,1}\right)_{eq}\sim N^2\exp(-2.3t/\tau_{nmode}), \tag{11}$$

(i.e. its time scale is identical to that of the polymer stress). Since, at long times, the chain shows negligible transverse evolution, we may conclude that only the longitudinal relaxation of the polymer chain contributes to the stress relaxation at these times. Similarly to the rest of the properties we have discussed in this paper, scaling arguments verify that the observed power law during intermediate times is the

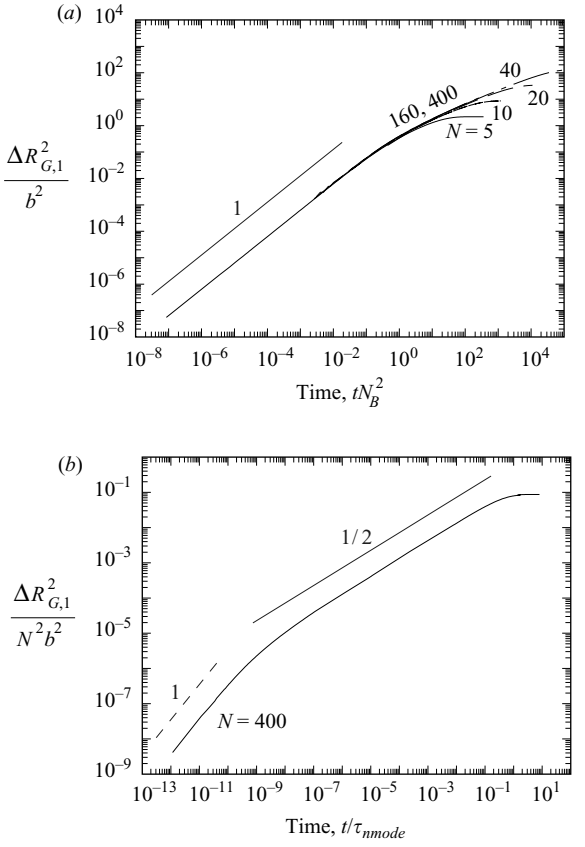

FIGURE 6. Longitudinal reduction of the polymer chain at (*a*) short times and (*b*) intermediate times. Note that we plot the difference $\Delta R^2_{G,1} \equiv R^2_{G,1}(0) - R^2_{G,1}(t)$. Both curves were generated by employing chains with $N = 5, 10, 20, 40, 160, 400$.

simplest power law which can match the conditions at the end of the short times and the beginning of long times. By requiring that

$$\left(\Delta R^2_{G,1}\right)_{short} = 1\,(tN^2)^a = \left(\Delta R^2_{G,1}\right)_{long} = N^2\left(\frac{t}{N^2}\right)^a, \tag{12}$$

we can easily derive that $a = 1/2$ and thus, at intermediate times, the length reduction is given by (10) above.

To investigate the rotation of the entire polymer chain, in figure 8 we plot the relaxation of the rotation function $\mathrm{Rot}(t) \equiv \langle \boldsymbol{U}(t) \cdot \boldsymbol{U}(0) \rangle$, where $\boldsymbol{U}$ is the unit end-to-end vector. We note that values of 1 result from polymer chains aligned in the '1' direction while values of 0 result from polymer chains with random orientations. At short and intermediate times, the chain is still aligned in the (original) '1' direction, while it starts to rotate at times $t \sim \tau_{nmode}$. As this figure clearly reveals, the rotational relaxation starts much later than the longitudinal relaxation (even though they both have the same long-time scaling). As depicted in figure 8(*b*), the rotational relaxation at long times follows an exponential decay $\approx \exp(-0.92\,t/\tau_{nmode})$. (The coefficient of $0.92 = 0.4 \times \ln 10$ is approximate owing to noise.)

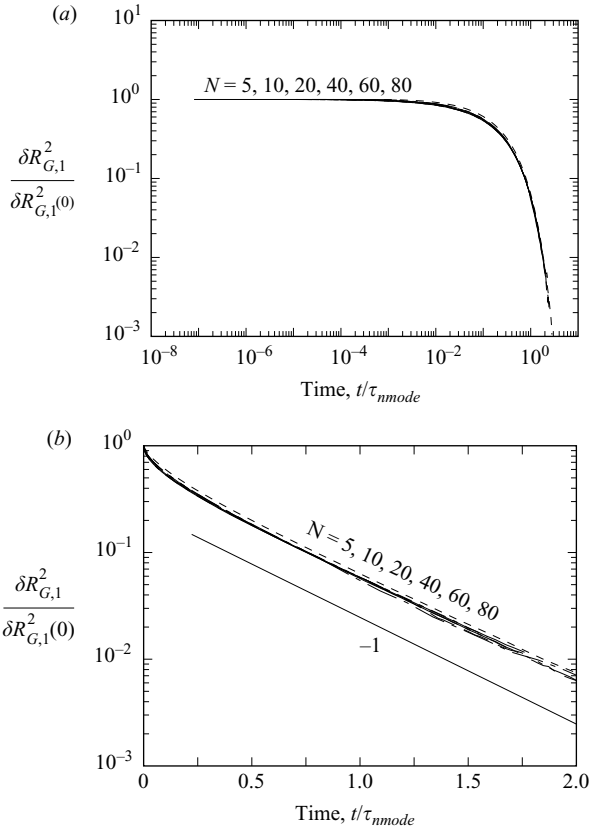

FIGURE 7. Longitudinal evolution of the polymer chain. (*a*) Scaling law for the evolution of the first eigenvalue $R^2_{G,1}$ of the gyration tensor at short and intermediate times for chain length $N = 5, 10, 20, 40, 60, 80$. Note that we plot the difference $\delta R^2_{G,1} \equiv R^2_{G,1}(t) - (R^2_{G,1})_{eq}$ (where $(R^2_{G,1})_{eq} = 0.76\,(R^2_G)_{eq}$ is the value of the first eigenvalue at equilibrium) scaled by the value of the difference at time $t = 0$, i.e. $\delta R^2_{G,1}(0) \equiv R^2_{G,1}(0) - (R^2_{G,1})_{eq}$. (*b*) Scaling law for the evolution of $R^2_{G,1}$ at long times for the same values of chain length N as in (*a*).

We end this section by considering the diffusion of the entire chain described by the motion of the polymer's centre of mass $\boldsymbol{X}_c$. Summing (1) over all beads, the sum of the corrective forces and the tensions is zero, resulting in a simple balance between the hydrodynamic force and the sum of the 'white noise' Brownian forces,

$$\zeta \frac{\mathrm{d}\boldsymbol{X}_c}{\mathrm{d}t} = \boldsymbol{F}^{rand}_c \equiv \frac{1}{N+1} \sum_{i=1}^{N+1} \boldsymbol{F}^{rand}_i. \tag{13}$$

Therefore, the centre of mass follows an ordinary diffusion

$$\langle (\boldsymbol{X}_c(t) - \boldsymbol{X}_c(0))^2 \rangle = 6\, D_C t, \tag{14}$$

with diffusivity $D_C = k_B T/(N+1)\zeta$. The diffusion of the chain's centre of mass produces an isotropic stress $-\boldsymbol{I}$ (where $\boldsymbol{I}$ is the unit 3×3 matrix) which is present at all times and is the only stress at equilibrium. We note that in Bird *et al.* (1987) the equation of motion for the centre of mass in the absence of hydrodynamic interactions and excluded-volume effects does not contain the Brownian force, which produces

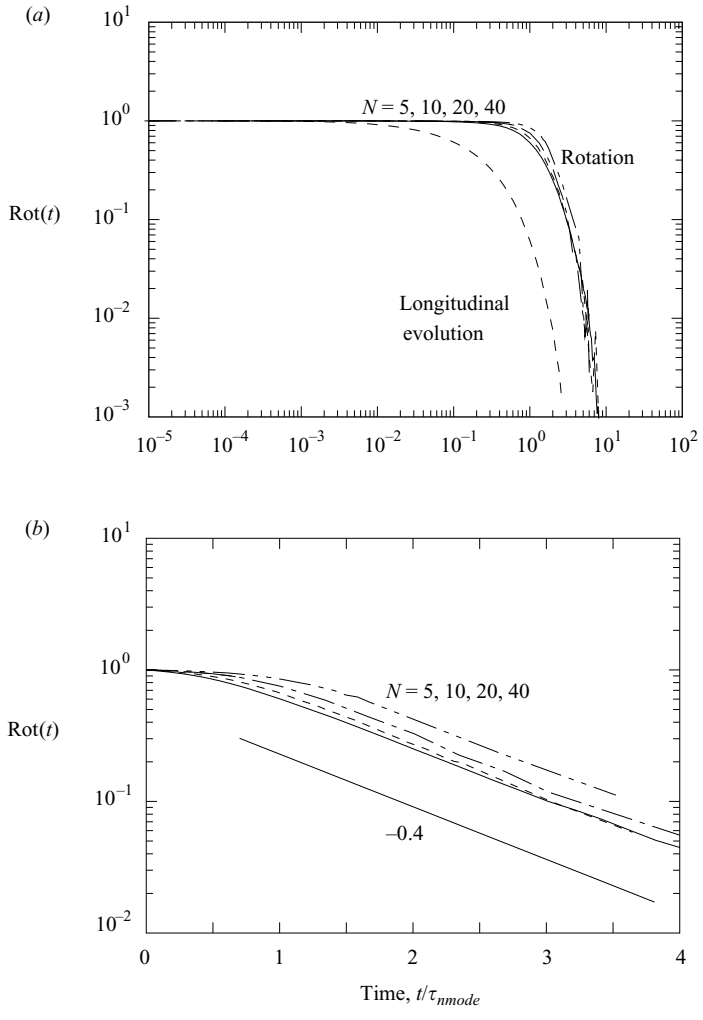

FIGURE 8. Rotational evolution of the polymer chain. (*a*) Evolution of the rotation function $\mathrm{Rot}(t) \equiv \langle \boldsymbol{U}(t) \cdot \boldsymbol{U}(0) \rangle$ (where $\boldsymbol{U}$ is the unit end-to-end vector) at short and intermediate times for chain length $N = 5, 10, 20, 40$. Also included is the longitudinal evolution of the polymer chain $\delta R^2_{G,1}/\delta R^2_{G,1}(0)$ from figure 7(*a*). (*b*) Evolution of the rotation function at long times for the same values of chain length N as in (*a*). (All curves fall as one if we scale $\mathrm{Rot}(t)$ with its scaling at the beginning of the rotation relaxation.)

a free diffusion in the absence of external forces; this error is repeated in several chapters of the book, e.g. see their equations (13.2-6), (14.2-5) and (15.1-2).

As a closure to this section, we note that a comparison of the evolution of the first and second eigenvalues (figures 5 and 6) with the stress relaxation shown in figure 3 reveals that the transition from the short-time to the intermediate-time behaviour and from the latter to the long-time behaviour occurs at exactly the same time for both functions. Thus, the evolution of the eigenvalues is a proper measurement of the configuration evolution for the entire chain and its impact on the stress relaxation.

5. Relaxation of a straight bead-rod chain: discussion

Based on our numerical results and the application of scaling laws, we now have a clear picture for both the stress relaxation and the configuration evolution from short up to long times. In summary, at short times $t \ll N^{-2}$, the chain's width grows as $R_\perp \sim t^{1/2}$ and its length is reduced as $R_\parallel(0) - R_\parallel \sim Nt$; at intermediate times $N^{-2} \ll t \ll N^2$, the corresponding values are $R_\perp \sim N^{-1/4} t^{3/8}$ and $R_\parallel(0) - R_\parallel \sim t^{1/2}$. During both short and intermediate times, the chain is practically straight, i.e. its length is $R_\parallel = O(N)$. At long times $t \geqslant N^2$, no transverse configuration relaxation is observed while the chain's length decays as $R_\parallel^2 - (R_\parallel^2)_{eq} \sim N^2 \exp(-2.3t/\tau_{nmode})$. Until late in long times the chain is practically aligned along the initial '1' direction; afterwards, the chain shows a rotational relaxation which follows an exponential decay similar to that for the longitudinal length. At all times, the centre of mass of the polymer follows a free diffusion with constant diffusivity $D_C = k_B T/(N+1)\zeta$. In addition, at short times, the strong stress component is $\sigma_{11} \sim N^3$ while the weak stress component is $\sigma_{22} = (N+1)$ (in absolute value since σ_{22} is negative). At intermediate times, the stress decay is anisotropic; $\sigma_{11} \sim N^2 t^{-1/2}$ while $\sigma_{22} \sim N^{1/2} t^{-1/4}$. Finally, at long times, the polymer stress shows an exponential decay towards equilibrium: $\sigma_{11} \sim N \exp(-2.3t/\tau_{nmode})$ and $\sigma_{22} \sim \exp(-2.3\,t/\tau_{nmode})$; thus, at times $t \sim \tau_{nmode} \sim N^2$, the two stress components still have different magnitudes: $\sigma_{11} = O(N)$ while $\sigma_{22} = O(1)$.

Throughout this section, we denote the longitudinal and transverse lengths of the chain as $R_\parallel$ and $R_\perp$, of the links as $d_\parallel$ and $d_\perp$, and the longitudinal and transverse positions of the beads (with respect to the chain's centre of mass) as $X_\parallel$ and $X_\perp$, respectively. (The longitudinal and transverse directions refer to the orientation of the entire chain.) We emphasize that for an elongated chain, the chain's width $R_\perp$ scales similarly to the transverse bead position $X_\perp$, while the chain's length $R_\parallel$ scales similarly to the sum of the longitudinal length $d_\parallel$ of all links, i.e. $R_\parallel \sim \sum d_\parallel$. In addition, owing to the link inextensibility, the transverse length $d_\perp$ of a link is associated with its longitudinal length $d_\parallel$, i.e. $d_\perp^2 = b^2 - d_\parallel^2$ where b is the fixed distance between two successive beads. Thus, properties which depend on $R_\parallel$, $d_\parallel$ or $d_\perp$ should scale with the chain's length, while those which depend on $R_\perp$ or $X_\perp$ should scale with the chain's width.

The conformational evolution for a typical polymer chain is shown in figure 9. The first few configurations show the transverse chain motion, while the last ones reveal the chain's longitudinal relaxation towards the equilibrium coil-like shape.

5.1. *Relaxation at short times*

Following the work of Grassia & Hinch (1996), at short times $t \ll N^{-2}$, the chain is almost straight and since $\sigma_{11} \sim N^3 \sim \sum T$ we may conclude that the tensions on each bead scale as $T \sim N^2$. Thus, at these times, the transverse component of the tension force on each bead is $F_\perp^{ten} \sim T d_\perp \sim N^2 t^{1/2}$ where $d_\perp \sim X_\perp \sim R_\perp \sim t^{1/2}$ owing to the transverse free diffusion. The transverse evolution of each bead scales similar to that of the entire chain, i.e. $X_\perp \sim R_\perp \sim t^{1/2}$; by combining this with the equation of motion, (1), we conclude that the transverse component of the Brownian force on each bead scales as $F_\perp^{rand} \sim t^{-1/2}$. At short times, $F_\perp^{ten} \ll F_\perp^{rand}$ and the dominant transverse Brownian force causes the beads to follow the free transverse diffusion shown in figure 5 as well as a constant weak stress component $\sigma_{22} \sim N X_\perp F_\perp^{rand} \sim N$ shown in figure 2(*b*). Thus, the transverse free diffusion and the associated longitudinal reduction are not able to produce any stress relaxation. During these times, the transverse tension force grows faster than the corresponding Brownian force. At

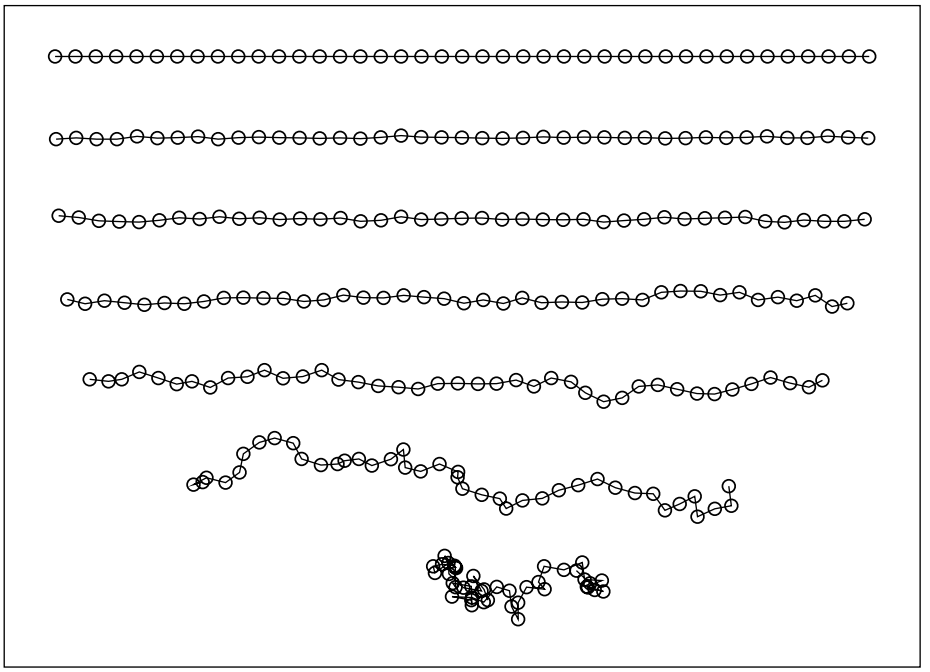

FIGURE 9. Typical chain configurations with $N = 40$ at times $t = 10^k\,\tau_{rand}$, where $k = -4, \ldots, 2$.

the transition times $t \sim N^{-2}$, $F_{\perp}^{ten} \sim F_{\perp}^{rand} \sim N$ and the free diffusion of the beads is arrested.

During short times, owing to the link inextensibility, the longitudinal length of each link shortens as $b^2 - d_{\parallel}^2 = d_{\perp}^2 \sim t$; this results in a chain's length reduction $R_{\parallel}^2(0) - R_{\parallel}^2 \sim N^2 b^2 - N^2 d_{\parallel}^2 \sim N^2 t$. Thus, the chain's length reduction shown in figure 6(*a*) results from the transverse bead diffusion and the link inextensibility.

The growth rate of the chain's width and the reduction rate of its length are

$$G_{\perp} \sim \frac{\mathrm{d}R_{\perp}}{\mathrm{d}t} \sim t^{-1/2}, \quad G_{\parallel} \sim \frac{\mathrm{d}(R_{\parallel}(0) - R_{\parallel})}{\mathrm{d}t} \sim N, \tag{15}$$

respectively. Therefore, the short times $t \ll N^{-2}$ denote a period of dominant transverse growth; this dominance is extended until the transition times $t \sim N^{-2}$ where the two rates show a similar scaling $G_{\perp} \sim G_{\parallel} \sim N$.

5.2. *Relaxation at intermediate times*

At intermediate times $N^{-2} \ll t \ll N^2$, the tensions on each bead are $T \sim N t^{-1/2}$ since the polymer is still practically straight while $\sigma_{11} \sim \sum T \sim N^2 t^{-1/2}$. We have verified the scaling of the tensions numerically by calculating the average tensions among the beads over the same time period as the polymer stress. (Also note that these tensions match at the transition times $t \sim N^{-2}$ the tensions valid at short times.) Therefore, the intermediate times are associated with a relaxation of tensions (necessary to ensure link inextensibility) from a magnitude of $T = O(N^2)$ at times $t = O(1/N^2)$ to a magnitude of $T = O(1)$ at times $t = O(N^2)$.

At these times, the strong stress component σ_{11} shows the same decay law ($t^{-1/2}$) as that near equilibrium (Dimitrakopoulos *et al.* 2001). We emphasize that this

is a mere coincidence. The flexible chain during intermediate times is far from equilibrium: the polymer is still practically straight since its longitudinal length is $R_\parallel = O(N)$ (as shown in figure 7*a*), while at the beginning of the intermediate times the magnitude of the strong stress is $\sigma_{11} = O(N^3)$, much greater than the magnitude of the stress near equilibrium. This conclusion is also obvious if we consider that the weak stress component σ_{22} shows a different power-law decay at these times, i.e. $t^{-1/4}$.

During intermediate times, the participation of the different length scales in the polymer relaxation results in a slower transverse growth $R_\perp \sim N^{-1/4} t^{3/8}$ as well as in a slower longitudinal reduction $R_\parallel(0) - R_\parallel \sim t^{1/2}$ compared to those at short times. The growth rate of the chain's width and the reduction rate of its length are now

$$G_\perp \sim \frac{\mathrm{d}R_\perp}{\mathrm{d}t} \sim N^{-1/4}\, t^{-5/8}, \quad G_\parallel \sim \frac{\mathrm{d}(R_\parallel(0) - R_\parallel)}{\mathrm{d}t} \sim t^{-1/2}, \tag{16}$$

respectively. At intermediate times $G_\parallel \geqslant G_\perp$ and thus, with respect to the entire chain, these times denote a period of dominant longitudinal reduction. By comparing the link longitudinal and transverse growth rates, Grassia & Hinch (1996) have shown that the motion of the links is primarily transverse at these times. The difference between the links and chain relaxation may be attributed to the participation of the different relaxation modes, as discussed at the end of this subsection.

Based on the understanding that the intermediate times denote a period of dominant longitudinal reduction, it is natural to seek a mechanism associated with the longitudinal direction of the polymer relaxation. In particular, consider that the length reduction of the polymer chain reveals the longitudinal component of the force acting on the entire chain

$$F_\parallel \sim \zeta_{ch} \frac{\mathrm{d}\Delta R_\parallel}{\mathrm{d}t} \sim N t^{-1/2}, \tag{17}$$

where $\zeta_{ch} \sim N$ is the friction coefficient for the entire chain. This force is nothing other than the tension force along the polymer chain, $F_\parallel^{ten} \sim T\, d_\parallel \sim N t^{-1/2}$ since the tensions during intermediate times relax as $T \sim N t^{-1/2}$ while the polymer chain is still practically straight, i.e. $d_\parallel \sim 1$. Based on the above, the relaxation of the stress component σ_{11} at intermediate times results from the corresponding relaxation of the polymer length. In particular, by considering the entire chain or summing over all beads, we obtain

$$\sigma_{11} \sim R_\parallel\, F_\parallel \sim N d_\parallel\, F_\parallel \sim N^2 t^{-1/2}, \tag{18}$$

(where we use $R_\parallel \sim N$ and $d_\parallel \sim 1$) which agrees with the results shown in figure 3(*a*).

The chain's length reduction and the corresponding longitudinal force satisfy the equipartition of energy, i.e. $F_\parallel\, \Delta R_\parallel \sim N k_B T$, which reveals that during intermediate times there exists a quasi-steady equilibrium in the longitudinal direction. We note that although in this paper we focus on the chain's longitudinal relaxation, the proposed mechanism is identical to that found in Grassia & Hinch (1996) based on a sideways motion model. To explain this, observe that the chain's length reduction is associated (owing to the link inextensibility) with a transverse link growth $d_\perp^2 \sim N^{-2}\,(R_\parallel^2(0) - R_\parallel^2) \sim N^{-1} t^{1/2}$ and thus, the transverse link growth is connected with the tensions T via the relation $d_\perp^2 \sim T^{-1}$ as found in GH by assuming a quasi-steady solution in their sideways motion model. (We note that we have verified numerically the transverse link growth $d_\perp^2 \sim N^{-1} t^{1/2}$ by monitoring several links along a chain with $N = 160$.)

The longitudinal mechanism is in agreement with the recent results of Ghosh *et al.* (2001) where the longitudinal force along a Cramer's chain was numerically determined as a function of the chain length and was shown to follow the predictions of the FENE model during relaxation. To explain this, we have to consider that for a practically straight chain (as in our problem until the end of the intermediate times) the FENE model predicts a (longitudinal) force identical to that for a bead-rod chain with the same extension,

$$F^{FENE} = \frac{HQ}{1 - Q^2/Q_o^2} \sim \frac{N^2}{R_\parallel^2(0) - R_\parallel^2} \sim Nt^{-1/2}, \tag{19}$$

where the proportionality constant H scales as $H \sim N^{-1}$, $Q_o \sim N$ is the maximum extension, Q is the end-to-end distance while we use $R_\parallel^2(0) - R_\parallel^2 \sim Nt^{1/2}$ from (10) above. This coincidence results from the fact that the FENE model is based on the assumption that the chain can sample all configurations for a given end-to-end distance, i.e. the configuration distribution function has come to equilibrium. Therefore, the FENE assumption is in agreement with the quasi-steady equilibrium of the bead-rod chain during relaxation. We emphasize that the discussion above shows that a FENE dumbbell is able to predict the correct longitudinal relaxation of the entire chain, but not the polymer's transverse relaxation. (Furthermore note that a dumbbell cannot physically represent the relaxation of an initially straight chain; the latter should be discretized at least as a trimmer so that the chain has the ability to relax from the straight configuration to the coil-like one.)

Considering the transverse relaxation at intermediate times, we may conclude that the relaxation of the stress component σ_{22} results from the relaxation of the width of the polymer chain. In particular, the transverse evolution of the polymer chain, $R_\perp \sim X_\perp \sim N^{-1/4}t^{3/8}$, is associated with a dominant transverse force on each bead $F_\perp \sim \zeta \, \mathrm{d}X_\perp/\mathrm{d}t \sim N^{-1/4}t^{-5/8}$; both produce a stress decay $\sigma_{22} \sim N X_\perp F_\perp \sim N^{1/2}t^{-1/4}$ in agreement with the results shown in figure 3(*b*).

The growth $t^{3/4}$ of the chain's width at intermediate times may be attributed to the participation of the different relaxation modes. In particular, if the chain were to relax transversely with only the longest mode, then the width evolution would be $(R_\perp^2)_{LM} \sim R_\parallel^2(0) - R_\parallel^2 \sim Nt^{1/2}$, which obviously overestimates the true width evolution as well as the value of $R_\perp^2$ at the end of the intermediate times (the longest mode predicts a final value $(R_\perp^2)_{LM} \sim N^2 \gg N$). On the other hand, if the chain were to relax transversely with only the shortest mode, the width evolution would be $(R_\perp^2)_{SM} \sim d_\perp^2 \sim b^2 - d_\parallel^2 \sim N^{-2}(R_\parallel^2(0) - R_\parallel^2) \sim N^{-1}t^{1/2}$, which underestimates the true width evolution. The participation of the different modes in the transverse relaxation results in a relaxation rate between the two extreme rates of the shortest and longest modes.

Proceeding further, we may conclude that at the beginning of the intermediate times $t \sim N^{-2}$ the chain relaxes transversely with its smallest mode only due to the short-time transverse free diffusion (i.e. $R_\perp^2 \sim d_\perp^2$). As the time increases, longer modes participate in the chain relaxation. At the end of intermediate times, the chain does not relax with its longest mode only, but some other (long) modes also participate in the relaxation. This conclusion is supported by the observation that, at times $t \sim N^2$, the chain is still practically straight, i.e. $R_\parallel^2 = O(N^2)$ even though the chain's width has reached its scale at equilibrium, $R_\perp^2 = O(N)$. (If the chain were relaxing at times $t \sim N^2$ with only its longest mode while being practically straight, its width would be $R_\perp^2 \sim R_\parallel^2(0) - R_\parallel^2 \sim N^2 \gg N$.)

To provide a qualitative picture of the mode relaxation, we may determine the evolution of the average relaxation mode by replacing the contribution of the different modes by a single mode with a time-dependent length and amplitude. The transverse growth of such a mode is the same as that for the entire chain, i.e. $R_\perp$, while the link inextensibility at the mode wave results in a time-dependent wavenumber N_M which should follow the requirement $R_\perp^2 \sim N_M^{-2}(R_\parallel^2(0) - R_\parallel^2)$ or $N_M \sim N^{3/4} t^{-1/8}$. Thus, the wavenumber of the average mode decreases with time, from $N_M \sim N$ at times $t \sim N^{-2}$, to $N_M \sim N^{1/2}$ at times $t \sim N^2$, i.e. the mode's wavelength increases with time from $R_\parallel^M \sim 1$ at $t \sim N^{-2}$ to $R_\parallel^M \sim N^{1/2}$ at $t \sim N^2$. This analysis verifies our previous conclusions on the mode relaxation. The different (long) modes which participate in the chain's relaxation at the end of intermediate times are expected to decay afterwards and may be responsible for the specific relaxation rate of the bead-rod model during the transient long times.

5.3. *Relaxation at long times*

At the end of the entire relaxation, the polymer chain is expected to have reached equilibrium; thus, the following question arises: how close to equilibrium is the polymer chain during the (transient) long times? Looking carefully at figure 7(*b*), it is clear that, at the beginning of the exponential decay, the polymer length is still of magnitude $R_\parallel^2 = O(N^2)$, i.e. the chain is still practically straight. In addition, the entire exponential decay shown in figure 7(*b*) has not significantly changed the polymer length. (This is especially true if we consider that the behaviour shown in this figure is a scaling law valid even for very large N). Thus, during the long times of the transient dynamics, the chain is still far from equilibrium. This conclusion is also supported by the magnitude of the strong stress component at the beginning of long times; figure 4(*a*) shows that $\sigma_{11} = O(N)$, much greater than its equilibrium values $(\sigma_{11})_{eq} = O(1)$.

Therefore, only near the end of the long-time behaviour of transient dynamics is the chain close to equilibrium, where it obtains a coil-like shape. By requiring that the chain is close to equilibrium when $R_{G,1}^2(t) - (R_{G,1}^2)_{eq} \ll (R_{G,1}^2)_{eq}$, the exponential decay of the chain's length shown in figure 7(*b*) leads to $t \gg N^2 \ln N$, i.e. the times $\sim N^2 \ln N$ denote the transition from the nonlinear to the linear dynamics for the problem studied in this paper. We emphasize that monitoring transient properties near equilibrium produces results indistinguishable from the noise of the Brownian motion (especially when no variance reduction technique is employed, as happens in our study.)

Even though the polymer has not reached the linear regime at the transient long times, its behaviour at these times is similar to the corresponding behaviour near equilibrium. Both processes are associated with the relaxation of the chain's longitudinal length. Thus, they both begin at times $t \sim \tau_{nmode} \sim N^2$ and show an exponential decay with time scale a multiple of τ_{nmode}, i.e. the time scale associated with the entire polymer chain. In addition, for both problems, the stress decay rate is twice that of the longitudinal length. Therefore, the polymer behaviour at the transient long times could be explained similarly to that for the linear relaxation. In particular, observe that $\sigma_{11} \sim \sum d_\parallel F_\parallel$ where $d_\parallel$ is the longitudinal separation of adjacent beads $d_\parallel \sim R_\parallel / N \sim \exp(-1.15t/\tau_{nmode})$, and $F_\parallel$ is the force acting on the link (or bead). Because of the exponential decay in $d_\parallel$, the corresponding force $F_\parallel$ is linear to $d_\parallel$, similarly to what happens near equilibrium. Thus, $\sigma_{11} \sim N \exp(-2.3t/\tau_{nmode})$, in agreement with our numerical results. We could also explain the polymer behaviour considering the entire chain length. In this case, $\sigma_{11} \sim R_\parallel F_\parallel$ where now $F_\parallel$ is the force

acting on the entire chain $F_{\|} \sim R_{\|}/N$ based on the entropic model, and we find again the correct stress scaling $\sigma_{11} \sim N \exp(-2.3\, t/\tau_{nmode})$. While these explanations predict the correct scaling for the strong stress component σ_{11}, they fail to predict the correct magnitude for the weak stress component σ_{22}. This failure is another indication that, although similar to linear relaxation, the long time relaxation of an initial straight chain is still nonlinear, i.e. far from equilibrium. In addition, it shows that knowledge of the entire polymer stress (i.e. both stress components) helps us to understand the polymer relaxation better.

6. Comparison with experimental results on DNA relaxation

As a closure to this study, we compare our computational results with the experimental findings from the work of Perkins *et al.* (1994). In that study, single DNA molecules 4 to 43 μm long were stretched to full extension in a flow field, and their relaxation was measured when the flow stopped. The molecules were manipulated by attaching a 1 μm polystyrene sphere at one end of the chain and employing optical tweezers. We note that the relaxation of a tethered chain is not the same as that of a free chain (the tethered relaxation nearly corresponds to a free relaxation with twice the chain length); nevertheless, here we attempt a comparison with our results.

The shapes of DNA molecules shown in figure 2(*a, b*) of the experimental study are qualitatively similar to the shapes of the half portion of the molecules from our study (figure 9). The DNA molecules also reveal limited rotation even at long times, as reported in our study. In addition, in the experimental work, the visual length of DNA molecules was measured after the flow was turned off and was found to exhibit a single exponential decay at long times, qualitatively similar to that found in our study.

In quantitative terms, Perkins *et al.* reported that the longest relaxation time increases with the polymer length as $\tau_{DNA} \sim N^{1.66 \pm 0.10}$. (We emphasize that they measured the visual length of the polymer and not the more relevant length squared). Further reading of the experimental study reveals that Perkins *et al.* also employed dynamic scaling with three length templates and found that the scaling exponent increases with increasing length; the longest length templates ($L = 41\,\mu$m) gave a time scale $\tau_{DNA} \sim N^{1.79 \pm 0.08}$. The authors reported that these templates may be more indicative of the true value of the scaling exponent because the corresponding data were better and contained more information. The same experimental group reported that longer chains reveal higher scaling exponents in a study on the hydrodynamics of a DNA molecule in a flow field as well (Larson *et al.* 1997).

Therefore, it is unclear what the true exponent is for the longest relaxation time of DNA. It is also unclear what the influence of the tethered end is. (The same experimental group reported the longest time scale for free DNA relaxation, but unfortunately they did not report on the scaling exponent (Perkins *et al.* 1999)). Nevertheless, assuming that the true value falls between those predicted by the Rouse and Zimm theories, this finding could be explained by our results. In particular, our study suggests that the long-time chains of the experimental work may still be far from equilibrium, similar to our long-time numerical results. Thus, hydrodynamics interactions may also not be so important for the experimental study; this could produce an exponent between those predicted by the two theories. Of course, our conclusion can only be verified or rejected through further experimental and computational studies.

7. Conclusions

In this paper, we studied the conformational and stress relaxation of an initially straight flexible polymer by employing Brownian dynamics simulations based on a discrete flexible wormlike chain model. We duplicated the numerical results for the strong stress component σ_{11} of previous studies (Grassia & Hinch 1996; Doyle *et al.* 1997, 1998) over extended time periods through the use of scaling laws. The entire relaxation of the weak stress component σ_{22} was also presented over the same extended times. Studying the entire stress tensor helps us understand the polymer behaviour better; for example, the anisotropy in the polymer stress relaxation at intermediate times helped reveal the corresponding anisotropy in the configuration relaxation.

The stress relaxation was accompanied by the transverse and longitudinal relaxation of the polymer chain over the same extended time periods. To achieve this, we determined numerically the dynamic evolution of the eigenvalues of the gyration tensor; their evolution was shown to be an appropriate measurement of the configuration evolution for the entire chain and its impact on the stress relaxation. The configuration relaxation was shown to be anisotropic at intermediate times: the chain's length is reduced as $R_{\parallel}(0) - R_{\parallel} \sim t^{1/2}$ while its width is increased as $R_{\perp} \sim N^{-1/4} t^{3/8}$. By focusing on the chain's longitudinal relaxation, a quasi-steady equilibrium of the link tensions in shown to exist along the chain's length; the mechanism is identical to that found in Grassia & Hinch (1996) based on a sideways motion model. This mechanism also explains the ability of the FENE model to describe the longitudinal relaxation of the flexible bead-rod chain. In addition to the transverse and longitudinal relaxation, the rotation of the entire chain and the motion of its centre of mass were studied. The former was shown to be significant only late at long times (in agreement with experimental observations on DNA relaxation) while the latter follows a free diffusion at all times. The entire relaxation described in this article including the (transient) long-time behaviour was shown to be far from equilibrium.

By monitoring the evolution of the eigenvalues of the chain's gyration tensor and applying the scaling law methodology, the configuration relaxation was determined over extended time periods. Knowledge of the conformational behaviour helps us understand the polymer properties including the polymer stress. Thus, we believe that the methodology we developed for monitoring the polymer configuration is well suited to studying other problems in the area of polymer rheology.

The author of this paper would like to thank Professor Hinch for valuable discussions and suggestions on the relaxation mechanism. Helpful discussion with Professors Anisimov and Dorfman is also acknowledged. This work was supported by the Minta Martin Research Fund at the University of Maryland. The computations were performed on multiprocessor computers provided by the National Centre for Supercomputing Applications in Illinois (grant DMR000003), and by an Academic Equipment Grant from Sun Microsystems Inc.

REFERENCES

Bird, R. B., Curtiss, C. F., Armstrong, R. C. & Hassager, O. 1987 *Dynamics of Polymeric Liquids: Volume 2, Kinetic Theory*. John Wiley.

Dimitrakopoulos, P., Brady, J. F. & Wang, Z.-G. 2001 Short- and intermediate-time behavior of the linear stress relaxation in semiflexible polymers. *Phys. Rev.* E **64**, 050803(R).

Doi, M. & Edwards, S. F. 1986 *The Theory of Polymer Dynamics*. Clarendon.

Doyle, P. S., Shaqfeh, E. S. G. & Gast, A. P. 1997 Dynamic simulation of freely draining flexible polymers in steady linear flows. *J. Fluid Mech.* **334**, 251–291.

Doyle, P. S., Shaqfeh, E. S. G., McKinley, G. H. & Spiegelberg, S. H. 1998 Relaxation of dilute polymer solutions following extensional flow. *J. Non-Newtonian Fluid Mech.* **76**, 79–110.

Ghosh, I., McKinley, G. H., Brown, R. A. & Armstrong, R. C. 2001 Deficiencies of FENE dumbbell models in describing the rapid stretching of dilute polymer solutions. *J. Rheol.* **45**, 721–758.

Grassia, P. S. & Hinch, E. J. 1996 *J. Fluid Mech.* **308**, 255–288 (referred to herein as GH).

Fixman, M. 1978 *J. Chem. Phys.* **69**, 1527–1537.

Kranbuehl, D. E. & Verdier, P. H. 1977 Relaxation of the aspherical shapes of random-coil polymer chains. *J. Chem. Phys.* **67**, 361–365.

Larson, R. G., Perkins, T. T., Smith, D. E. & Chu, S. 1997 Hydrodynamics of a DNA molecule in a flow field. *Phys. Rev.* E. **55**, 1794–1797.

Perkins, T. T., Quake, S. R., Smith, D. E. & Chu, S. 1994 Relaxation of a single DNA molecule observed by optical microscopy. *Science* **264**, 822–826.

Perkins, T. T., Smith, D. E. & Chu, S. 1999 Single polymers in elongational flows: dynamics, steady-state and population-averaged properties. In *Flexible Polymer Chains in Elongational Flow* (ed. T. Q. Nguyen & H.-H. Kausch). Springer.

Wuite, G. J. L., Smith, S. B., Young, M., Keller, D. & Bustamante, C. 2000 Single-molecule studies of the effect of template tension on T7 DNA polymerase activity. *Nature* **404**, 103–106.

Yamakawa, H. 1997 *Helical Wormlike Chains in Polymer Solutions*. Springer.